Arab J Sci Eng (2016) 41:55–65
DOI 10.1007/s13369-014-1516-6

RESEARCH ARTICLE - CHEMISTRY

Comparative Study of Electrical Conductivity on Activated Carbons Prepared from Various Cellulose Materials

T. Adinaveen · J. Judith Vijaya · L. John Kennedy

Received: 18 June 2014 / Accepted: 31 October 2014 / Published online: 29 November 2014

Abstract The objective of this study was to calculate the electrical conductivity of the activated carbons obtained from various cellulose materials (sugarcane bagasse, rice straw, cotton cloth and waste newspaper) by a two-stage process. The DC conductivity was calculated by a two-probe method. Scanning electron microscopy and X-ray analysis confirmed the surface morphology and formation of graphene multilayer, respectively. The carbonization temperature has a distinct effect on the electrochemical performances of the cellulose materials. The activated carbon compressed at 750.12 kPa offered the highest electrical conductivity for all the other samples. It may be due to the dense packing of the material, collapse of the pores and decrease in air gap between the carbon particles as well as a combination of multilayer graphene, which could be the factors accountable for the increase in conductivity with compression pressures. The conductivity increases with an increase in the temperature. In addition, all the carbon samples showed a good electrochemical property and the specific capacitance at the scan rate of 2–3 mV/s.

Keywords Cellulose materials · Activated carbon · H_3PO_4 activation · Hierarchical porous carbon · Electrical conductivity

T. Adinaveen · J. J. Vijaya (✉)
Catalysis and Nanomaterials Research Laboratory,
Department of Chemistry, Loyola College, Chennai 600 034, India
e-mail: jjvijayaloyola@yahoo.co.in; jjvijaya78@gmail.com

T. Adinaveen
e-mail: adinavee@gmail.com

L. J. Kennedy
Materials Division, School of Advanced Sciences,
Vellore Institute of Technology (VIT) University,
Chennai Campus, Chennai 600 127, India

1 Introduction

Carbon has been known as an important element for more than a century. Carbon can be represented in many forms. The most distinguished forms of carbon include mainly diamond, graphite and charcoal [1]. In the past decade, porous carbons (PC), graphite, graphene and carbon nanotube have shown an intense effect on various applications, due to their distinctive properties, including mechanical, optical, electrical and electrochemical characteristics [2]. Electrical transport properties of PC have been widely studied in the beginning of 1990s for its potential applications in nanoelectronic devices [3]. However, most of the reports are focusing on their application relied on the nano-microscale characteristics, but only few of them have reported on their behaviour in macroscopic level. One of the significant phenomena is to study the effect of electrical conductivity on PC under different compression pressures. Sanchez Gonzalez et al. reported that the conductivity of PC increases with increase in compression pressure [2].

In general, increasing the compression pressure mechanically reduces the voids between the carbon particles, which on directly enhances the electrical contact. This may be correlated to the contact theory given by Mrozowski and Holm [4,5], they proposed that the electrical conductivity of a carbon black depends on the separation distance between each particle [6] and the average size [7]. It is well known that the size, arrangement, density and shape of the materials influence their electrical properties and their potential applications [8,9]. Hence, the production of carbon materials of a particular morphology is very significant for their various applications. Recently, there has been an ever-increasing interest in the preparation and processing of various nanostructured carbon materials proposed for prospective applications in supercapacitors [10], field emission [11], catalyst support [12] and solar energy conversion [13].

Currently, lignocellulose materials comprise of forestry, agricultural and agro-industrial wastes, which are easily available and contain high-value materials. These lignocellulose wastes are accumulated every year in large quantities [14]. These wastes are usually disposed by burning or by deposition in landfills, which cause brutal environmental harms, but conversion to higher-value products, such as, PC would be preferable. The preparation of PC from wastes is an example of how the high-value products are obtained from low-cost materials, simultaneously giving solutions to the problem of wastes materials [15–17]. Thus, the development of processes for recycle of these wastes is of great concern. These wastes are high in carbon contents and are very suitable for their use as raw materials in the preparation of PC. Such wastes include a variety of materials, such as sugarcane bagasse, switch grass, poplar trees, sawdust, brewer's spent grains, waste paper, stems, stalks, husks, leaves, shells and peels from cereals such as rice, corn, wheat, sorghum and barley, among others [18].

Preparation of PC involves mainly two steps. The first is the carbonization of raw carbonaceous materials in an inert atmosphere. Carbonization process is a phase to enrich the carbon content in carbonaceous substance by eliminating the non-carbon species, using thermal decomposition [19]. The second step is the activation of the carbonized product, using an activation agent. The objective of the activation process is to develop the pore volume, increase the diameter of pores and raise the porosity of activated carbon. During the first stage of activation process, unorganized carbon is separated, exposing the lignin to the action of activating agents and lead to the growth of microporous structure [20].

In our present work, the effect of the volume density of the compressed porous carbon on its electrical conductivity was investigated. The conductivity of carbon samples was measured by a two-probe technique. Effect of activation temperature on its conductivity was also reported. The temperature could affect the bulk density as well as its electrical conductivity. XRD analysis has confirmed the formation of graphitic carbon structure with lower crystallinity. The morphology of the porous carbons was investigated by scanning electron microscopy (SEM) studies. The obtained carbon shows excellent capacitance performance.

2 Materials and Methods

2.1 Preparation of Porous Carbons

The porous carbon was prepared in our laboratory by using sugarcane bagasse (SC), rice straw (RS), waste newspaper (WNP) and cotton cloth (CC) as the precursor materials by a two-stage process: precarbonization and chemical activation. In the precarbonization, the SC, RS and WNP carbons were heated at 400 °C at the rate of 5 °C per min for about 4 h and cooled down to room temperature at the same rate, whereas for CC, the cotton cloth was heated at 300 °C at the rate of 5 °C per min for about 3 h and cooled down to room temperature at the same rate. This is labelled as precarbonized carbon (PCC). The PCC is subjected to a chemical activation for the purpose of creating porous structure in the carbon matrix. In the chemical activation process, 50 g of the PCC was agitated with 250 g of aqueous solution containing 85 % H_3PO_4 by weight. The ratio of chemical activating agent/ PCC was fixed as 4:2. The chemical activant and PCC were homogeneously mixed at 85 °C for 4 h. After mixing, the PCC slurry was dried under vacuum at 110 °C for 24 h. The resulting samples were then activated in a vertical cylindrical furnace at a ?ow rate of 5 °C per min. This was followed by heating to three different activation temperatures 600, 700 and 800 °C, whereas for cotton cloth samples, 350, 400 and 450 °C at a heating rate of 5 °C per min using a programmer and maintained at a constant temperature for 1 h before cooling. After cooling, the activated carbons were washed successively with hot water for several times, until the pH became neutral and washed with cold water to remove the excess phosphorous compounds. The washed samples were dried at 110 °C to get the final product. The samples heated at three different activation temperatures 600, 700 and 800 °C, and cotton cloth samples at 350, 400 and 450 °C were labelled as SC 600, SC 700, SC 800, RS 600, RS 700, RS 800, WNP 600, WNP 700, WNP 800, CC 350, CC 400 and CC 450, respectively.

2.2 Electrical Conductivity Studies

The DC electrical conductivity (σ) was measured at room temperature by a two-probe technique. A gram of porous carbon was dried at 110 °C overnight was compressed in a hollow Pyrex glass cylinder with an inner diameter of 11 mm between two metal plungers at compression pressures ranging from 9.63 to 750.12 kPa. The top and the bottom of the plungers are made of copper metal. This is connected to a Keithly 614 electrometer to measure the DC electrical conductivity of the samples. The compression pressures throughout the measurements were maintained by placing the carbon-loaded metal plungers inside a compression pressure hydraulic press, 5 min were allowed before measuring any conductivity to avoid any transient effect of the sample reduction due to compression. The electrical conductivity was calculated using the following formula [21].

$$\sigma = \frac{L}{RA} \tag{1}$$

where L is the distance between the two pistons (cm), R, the electrical resistance (Ω) and A, the area of the piston surface (cm^2).

2.3 X-Ray Diffraction Studies

X-ray diffraction studies were performed using a Phillips X-pert diffractometer for 2θ values ranging from 10 to 80 °C using Cu K_α radiation at a wavelength of $\lambda = 1.540$ Å. The other experimental conditions included 1/2° divergence slits, a 5-s residence time at each step and intensity measurements in counts.

2.4 Surface Morphological Studies

Surface morphological measurements were taken on the samples using a Leo-JEOL scanning electron microscope. The carbon samples were coated with gold by a gold sputtering device for a clear visibility of the surface morphology.

2.5 Nitrogen Isotherms

N_2 adsorption–desorption isotherms of the activated carbon composites were measured using an automatic adsorption instrument (Quantachrome Corp., Nova-1000 gas sorption analyzer) for the determination of the surface area and the total pore volume.

2.6 Electrochemical Measurements

Electrodes were prepared by mixing 95 wt% activated carbon with 5 wt% polyvinylidenefluoride in ethanol to form a paste, and the slurry was coated onto the stainless steel plate, which serving as a current collector. The coated electrode was dried at 75 °C in a drying oven for 1 h to remove the organic solvents remaining in the micropores of the electrode, and then the electrode weight was measured to determine the amount of carbon coated on the stainless steel sheet. The typical mass of electrode material was found to be 0.5 mg. The electrochemical characterization of PCC, SC 600, SC 700, SC 800, RS 600, RS 700, RS 800, WNP 600, WNP 700, WNP 800, CC 350, CC 400 and CC 450 performed using Autolab model PGSTAT 302 N with three electrode systems. The carbon coated on the stainless steel sheet, Ag/AgCl and platinum wire was used as the working, reference and counter electrode, respectively. Cyclic voltammetry (CV) of these electrodes was performed in 1 M H_2SO_4 electrolyte.

2.7 Mechanism of EDLC Electrode Formation

An electrical capacitor (EDLC) consists of two porous polarizable electrodes. The energy-economy process in EDLC is realized by means of the division of the charge on the two electrodes with suitably large potential difference between them. The electric charge of an EDLC is determined by its capacitance. The electrochemical process in EDLC may be represented as follows:

On the positive electrode:

$$E_s + A^- \leftrightarrow E_s^+ // A^- + e^- \tag{2}$$

On the negative electrode:

$$E_s + K^+ + e^- \leftrightarrow E_s^- // K^+ \tag{3}$$

The overall reaction is

$$E_s + E_s + K^+ + A^- \leftrightarrow E_s^- // K^+ + E_s^+ // A^- \tag{4}$$

where E_s is the electrode surface area; // electrical double layer (EDL), where the charge is stored on its either side; K^+ and A^- cations and anions of the electrolyte, respectively.

In charging process, electrons are transferred from the positive electrode to the negative electrode through an external current source and ions from the volume of electrolyte move towards the electrodes. During discharging process, electrons shift from the negative electrode to the positive electrode through a load and ions return from the surface into the volume of electrolyte. Hence, during both charging and discharging process, the charge density at the interface and the electrolyte concentration alters. Theoretical notions concerning the specific (per unit true surface area of electrode) capacitance of EDL are based on the classic theories of EDL elaborated by Helmholtz, Stern, Gouy, Chapman, Grahame and others [22–24].

3 Results and Discussion

3.1 Electrical Conductivity Studies

Figure 1a–d shows the variation of the electrical conductivity (σ) of (a) sugarcane bagasse, (b) rice straw, (c) cotton cloth and (d) waste newspaper at 298 K (25 °C). The electrical conductivity of the activated carbon mainly depends on the measurement conditions. During the thermal treatment, the cellulose component of all the samples gets converted into carbon, whereas the pores are created as an effect of the release of volatile decomposition products. Submitting the carbon powder to pressure allows in raising the conductive phase relative volumetric fraction, and as a result, both the average number of contacts and the apparent electrical conductivity increase [31,32]. It is clear from Table 1 that the electrical conductivity at 9.63 kPa is low, signifying that the applied pressure is not sufficient to compress the pores or the air gap between the carbon particles. Hence, inter-particle electronic conduction becomes complicated. But the electrical conductivity is increased by threefold at 750.12 kPa as shown in Table 2. This is mainly due to the easy movement of the electrons from one particle to another facilitated by

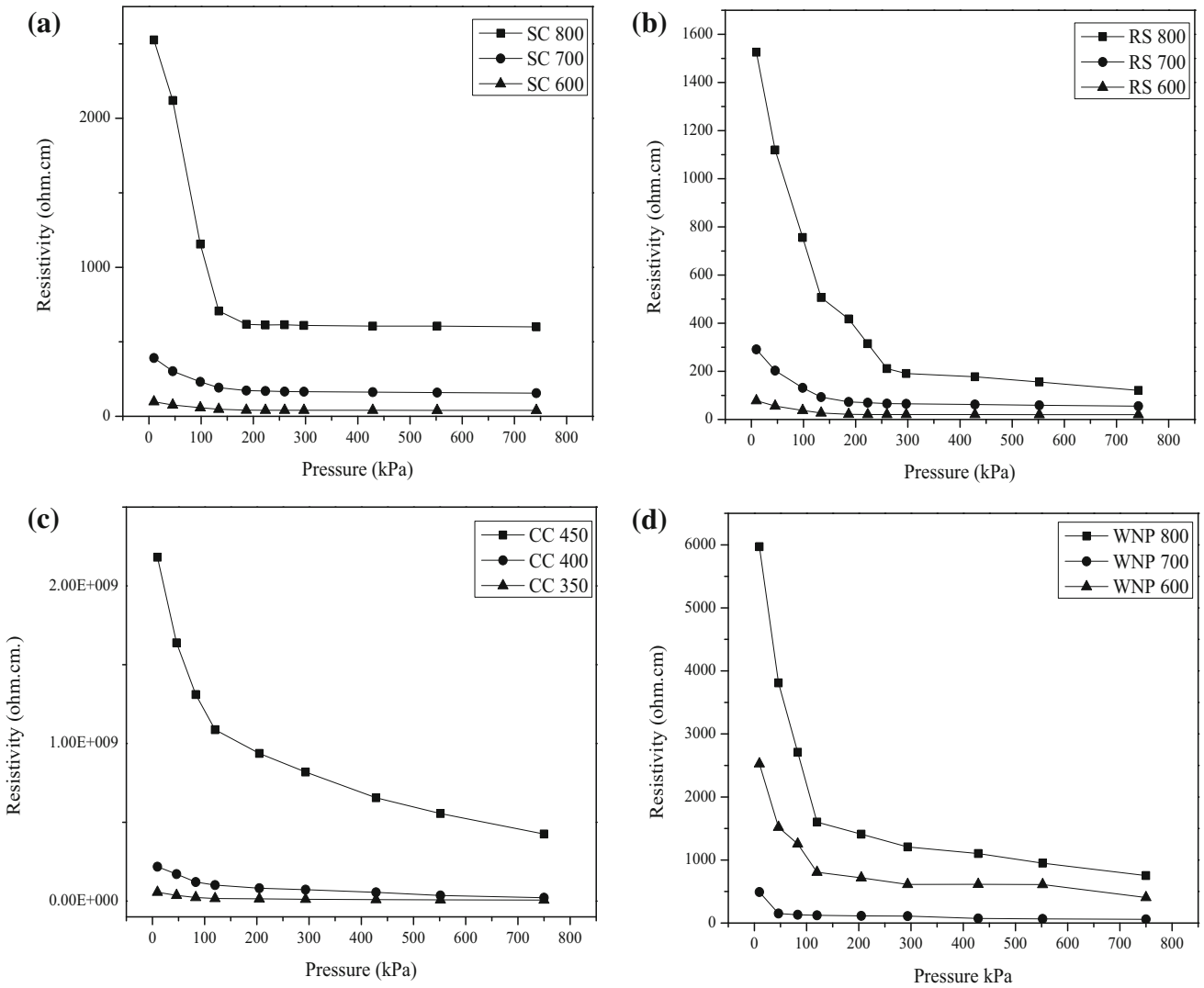

Fig. 1 Effect of compression pressure treatment on the electrical conductivity of the **a** SC, **b** RS, **c** CC and **d** WNP carbon samples

the removal of the air gap of the carbon by applying high pressure of compression. Thus, the electrical conductivity of the sample is supposed to be controlled by the compression pressure. In all the cases, the value of σ increases gradually with the compression exerted by the loadings. Higher density of carbon samples leads to higher electrical conductivity, because the probability for the electrons to move across them was high [25].

According to the contact theory proposed by Mrozowski and Holm [5], σ depends on the distance between the particles as well as their average size [9,26]. When pressure is applied, the aggregates are forced to be in a more intense packing arrangement, creating closer along with new contacts with neighbouring aggregates, as a result, the conductivity increasing. Although, pressure plays an important effect on σ, but it is not the only factor that changes its value. The morphology of the samples also shows an enormous effect on the electrical conductivity [27,28]. In case of PCC, the particles are irregular in shape and larger in comparison with the spherical particles of activation temperature as shown in Fig. 3a–h. It clearly shows that as the particle size increases, σ value and conductivity also steadily increases. Other properties of carbons, for instance the change in volume and density, due to compression, may also influence the value of σ [14].

Among sugarcane bagasse (a), rice straw (b), cotton cloth (c) and waste newspaper (d), the porous carbons having the highest conductivity are those prepared by using cotton cloth carbon as the precursor material. In cotton cloth, as the activation temperature increases, the electron could transfer all the way through the energy the barriers of the intersections easily and the conductivity increased to a great extent with the increase in activation temperature. As the conductivity values obtained for the cotton cloth carbon is relatively much

Table 1 Room temperature conductivities at a pressure of 9.63 kPa for different carbons

S. no.	Sugarcane bagasse		Rice straw		Waste newspaper		Cotton cloth	
	Sample	Room temperature conductivity (Ω^{-1} cm^{-1})	Sample	Room temperature conductivity (Ω^{-1} cm^{-1})	Sample	Room temperature conductivity (Ω^{-1} cm^{-1})	Sample	Room temperature conductivity (Ω^{-1} cm^{-1})
1	PCC	1.47×10^{-7}	PCC	1.33×10^{-7}	PCC	5.33×10^{-12}	PCC	4.22×10^{-7}
2	SC 600	1.90×10^{-4}	RS 600	1.53×10^{-5}	WNP 600	9.44×10^{-11}	CC 350	4.58×10^{-5}
3	SC 700	2.50×10^{-3}	RS700	2.20×10^{-4}	WNP 700	2.20×10^{-6}	CC 400	1.78×10^{-3}
4	SC 800	10.22×10^{-3}	RS 800	1.20×10^{-3}	WNP 800	2.83×10^{-3}	CC 450	1.22×10^{-1}

Table 2 Room temperature conductivities at a pressure of 750.01 kPa for different carbons

S. no.	Sugarcane bagasse		Rice straw		Waste newspaper		Cotton cloth	
	Sample	Room temperature conductivity (Ω^{-1} cm^{-1})	Sample	Room temperature conductivity (Ω^{-1} cm^{-1})	Sample	Room temperature conductivity (Ω^{-1} cm^{-1})	Sample	Room temperature conductivity (Ω^{-1} cm^{-1})
1	PCC	1.57×10^{-4}	PCC	1.93×10^{-5}	PCC	1.33×10^{-8}	PCC	2.01×10^{-4}
2	SC 600	18.90×10^{-4}	RS 600	16.10×10^{-5}	WNP 600	3.15×10^{-5}	CC 350	4.12×10^{-2}
3	SC 700	6.40×10^{-3}	RS700	6.10×10^{-4}	WNP 700	1.10×10^{-4}	CC 400	1.42×10^{-1}
4	SC 800	25.13×10^{-3}	RS 800	10.16×10^{-3}	WNP 800	5.86×10^{-2}	CC 450	$4.06 \times 10^{+10}$

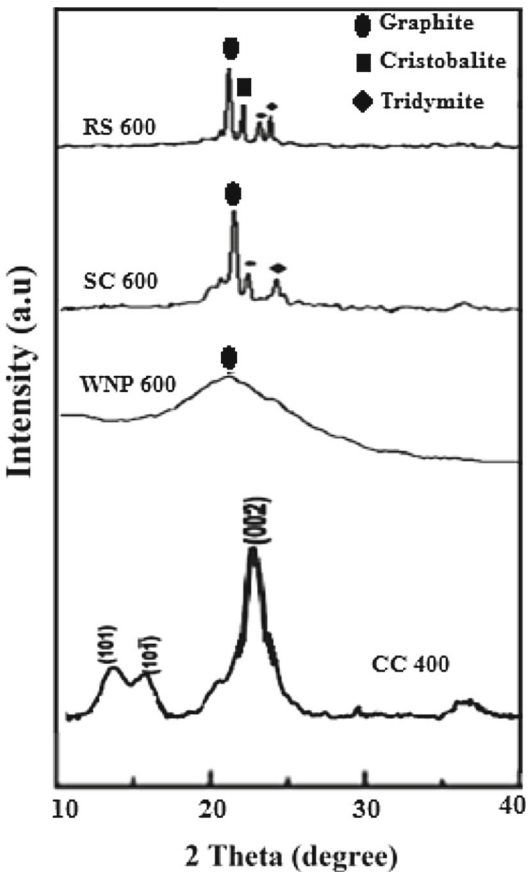

Fig. 2 X-ray diffraction pattern of SC 600, RS 600, CC 400 and WNP 600

higher, when compared to other carbons, the contribution to electrical conductivity in the composite is fully supposed to be due to the carbon matrix. This effect of temperature may come from graphitic structure, because the graphitic structure can be developed at higher temperature and transport higher conductivity [27].

3.2 X-Ray Diffraction Studies

Figure 2 shows the X-ray diffraction pattern of SC, RS, WNP and CC carbon prepared before and after H_3PO_4 treatment. The X-ray diffraction technique gives valuable information about the distribution of the active metal in the pore structure of the carbon support used in this study. The internal structure of the carbon matrix is considered to be the most important factor [29].

Both SC and RS consist of lignin, cellulose, hemicelluloses, ash content and volatile matters; however, RS contains an ash content of about 18.2 % (mainly silica), in an average, which is comparatively higher in comparison with other agricultural waste materials. RS is low in lignin along with high Si and K [30–32], which gives rise to a high content of SiO_2. The peaks corresponding to $2\theta = 23.18°$ show that the carbon can be regarded as a graphitized carbon. The peak observed at 24° corresponds to tridymite [33]. In addition, a sharp peak was observed at $2\theta = 26°$ and a very small one at $2\theta = 43°$ representing the formation of (0 0 2) and (1 0 0/1 0 1) planes corresponding to the graphitic structure. This shows

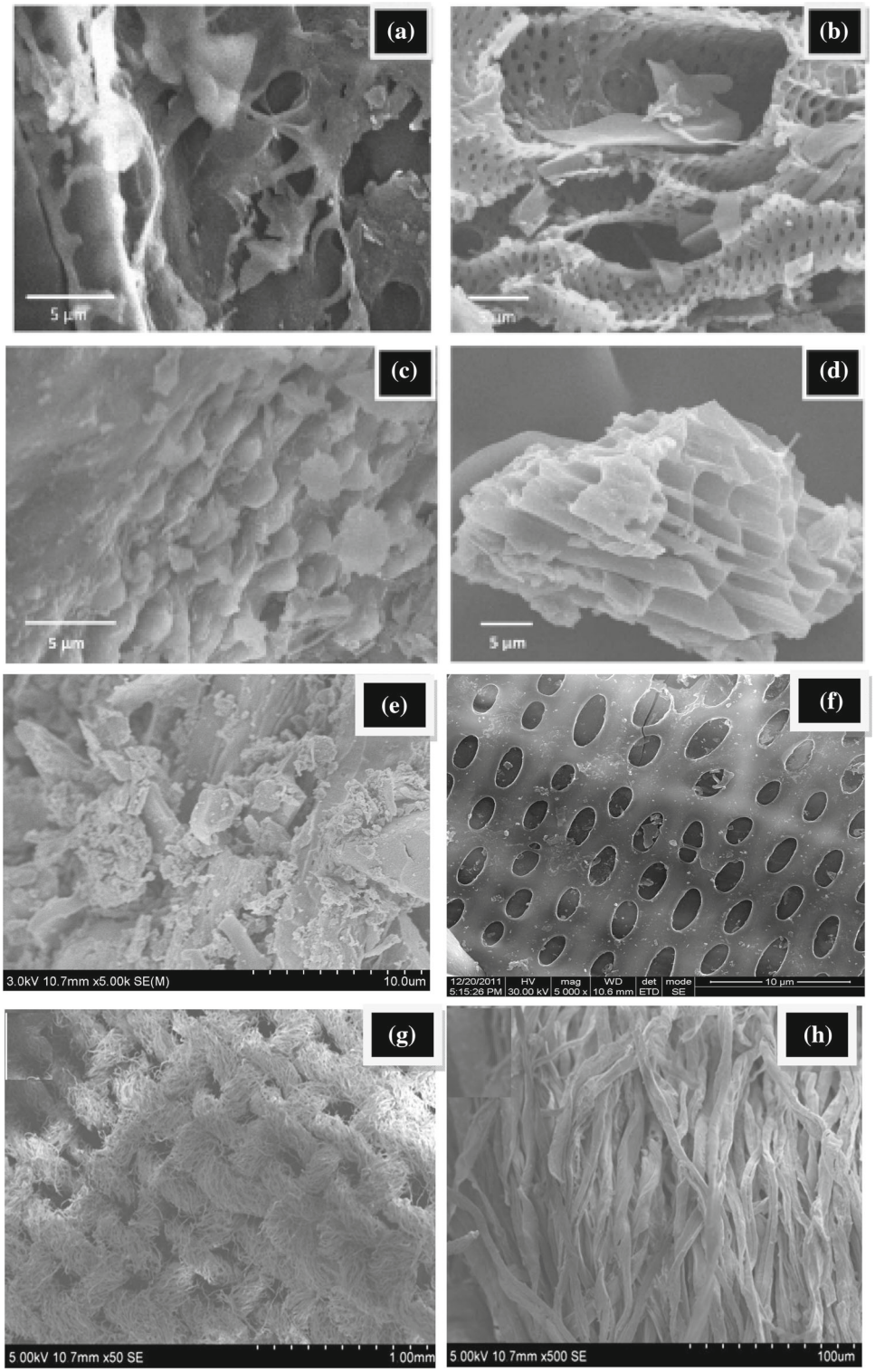

Fig. 3 SEM images of **a** SC PCC, **b** SC 600, **C** RS PCC, **d** RS 600, **e** WNP PCC, **f** WNP 600, **g** CC PCC and **h** CC 400

the development of atomic order and increase in crystallite size, which was accelerated by increasing the activation temperature. As the temperature varies from 600 to 800 °C, the peak becomes sharper and stronger, hence, indicating a better crystallization and increase in the crystallize size. The acid treatment along with activation temperature employed was responsible for the growth of crystalline structures.

Figure 2 shows the X-ray diffraction profiles of WNP carbon. The strong C (0 0 2) peak shows the graphitic carbon at 2θ (Cu K_α) of 23.1°, due to the hexagonal graphite struc-

ture, representing the turbostratic carbon structure through randomly oriented graphitic carbon layers [34]. In addition, peak around 43° may be due to the (1 0) bidimentional planes [35]. Thus, these results showed that all the carbon materials have a certain degree of graphitic structure, along with the decrease in the peak intensity, which indicates the amorphous state of the material. For cotton cloth, fibres were arranged in a systematic approach or lattice, although cotton cloth fabrics can be differentiated with their crystallinity. As reported in literature, unit cell of the CC is monoclinic with three principal places of reflection shown as (0 0 2), (1 0 1) and (1 0 1) [36]. Here also three peaks are found for cotton as shown (1 0 1) at $2\theta = 15°$, (1 0 1) at $2\theta = 16.4°$ and (0 0 2) at $2\theta = 22.7°$. All the above findings showed the formation of more stable graphitic carbon at higher temperature along with longer residence times.

3.3 SEM Studies

Figure 3a–d shows the SEM images of the SC and RS carbons before and after phosphoric acid activation. The surface morphology of PCC in Fig. 3a–c shows no formation of pores and confirms that only the lignocellulose portions present in SC and RS were changed to the carbon structures. The image also proves that only the carbonization has taken place. The sample activated at 600 °C showed better results, when compared with those activated at the other higher activation temperatures. The surface morphology was studied only for SC 600 and RS 600 sample alone, because of its high surface area. The SEM images of SC 600 and RS 600 are shown in Fig. 3b–d. The activation agents and activation temperature employed have created the pores on carbon surface. It has been made very clear that the opening of the pores in the surface at 600 °C have to be due to the extraction of some materials, e.g. dissolution of lignins and other mineral components from the straw and bagasse during the impregnation process, so as to create, upon activation, micro- and mesopores in the carbon along with silica components. As a result of the creation of pores, there is an increase in both the surface area as well as the pore volume, which are stably created in the carbon composite [37].

Figure 3e shows the SEM image of PCC, which shows no pores and confirms that only kaolinite, talc and cellulose portions present in WNP were converted to the carbon structures [37]. The image also shows that only the carbonizations have taken place. It is clear that due to some partial defects, large amount of silica has been etched away during the carbonization process. The surface morphology was studied only for the sample WNP 600 (Fig. 3f). In this image, porous structures with many cavities were observed. This cavity may be attributed due to the evaporation of the activating agent, which leaves space during carbonization, as well as the successive removal of untreated H_3PO_4 by washing with water [38]. From the Fig. 3f, hierarchical pores can be clearly identified. It clearly shows that the pores are more uniformly distributed, compact and there is a good network of interconnected pores in the mesoporous range. WNP 600 has a well-developed interconnected hierarchical pore system contain both micropores and mesopores.

Figure 3g, h shows the SEM image of PCC and CC 450. It shows the original morphology and fibres integrity of the precursors. However, the CC 450 presented certain reduction due to the carbonization process, as could be inferred from the relative reduction in fibre's diameter. It was postulated that extensive H_3PO_4 activation changes the nature of the carbon substrate drastically in the amorphous portions that are shattered to give a large pore volume, while the pore entrances become organized graphitic regions. Water molecules apparently can go through more easily into the pore system, because of the precise hydrogen-bonding interactions [39].

3.4 Adsorption/Desorption Isotherms

Nitrogen adsorption analysis at 77 K was carried out to examine the changes in the specific surface area and pore texture of the PCC and ACC of the cellulose carbons followed by phosphoric acid treatment under different conditions. Table 3 summarizes the textural properties of SC 600, RS 600 WNP 800 and CC 400, having the highest surface area among the other samples, for which meso- and microporous surface areas are comparable. The BET surface area of the SC 600 and RS 600 increases with increase in the activation temperature. This may be attributed to the creation of slit or cylindrical pores covering both the microporous and mesoporous ranges and shall be attributed to the pores generated on both carbon and silica components. The decrease in the surface area for SC 700, SC 800, RS 700 and RS 800 compared to SC 600 and RS 600 could be due to the pore contraction or the activation agents probably deposited in the inner pores and voids of the carbon matrix. Activation of the sugarcane bagasse (SC) and rice straw (RS) carbon by phosphoric acid was generally more effective for introducing the mesopores in the pore width range of 3–8 nm. Phosphoric acid can enter into the interior of the SC carbon structure and freely facilitate the activation [40]. As a result, SC-activated carbon exhibited the larger mesopores carbon with a larger average pore diameter than RS activated carbon as shown in Table 3. Furthermore, increasing the activation temperature decreases the BET surface area. The mechanism is the blocking of pores by the ashes. At low activation temperature, the ashes are in the form of fine, well- dispersed particles that tend together at higher activation temperatures. With such a mechanism, more porosity is blocked at high activation temperature, thereby explaining why the surface area of the carbon decreases faster with increasing temperature as reported by Fierro et al. [41]. After the activation process,

Table 3 Surface properties of the cellulose carbons

Sample	Surface area (m^2/g)	Total pore volume (cm^3/g)	Micro-pore surface area (m^2/g)	Meso-pore surface area (m^2/g)	Average pore diameter (nm)
PCC (SC)	169.60	0.246	129.84	39.75	2.9
PCC (RS)	135.06	0.196	96.04	37.13	2.7
PCC (WNP)	336.09	1.088	293.01	40.07	1.9
PCC (CC)	581.34	0.518	522.07	59.23	1.2
SC 600	676.95	0.424	620.21	56.73	1.2
RS 600	376.65	0.324	330.19	46.03	1.0
WNP 800	1,104.08	1.258	563.71	503.39	1.2
CC 400	1,193.17	1.279	573.89	579.8	0.9

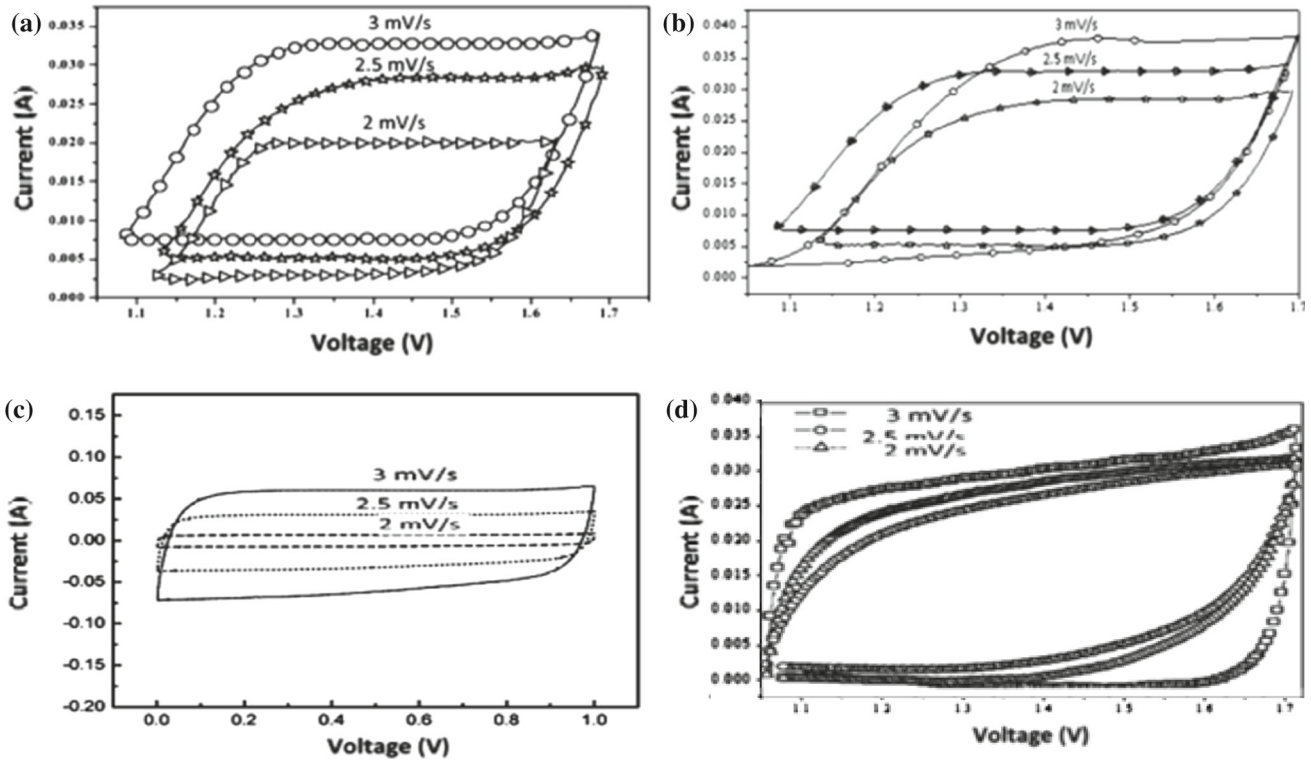

Fig. 4 Cyclic voltammogram of **a** SC 600, **b** RS 600, **c** CC 400 and **d** WNP 600 carbon samples at a scan rate of 2–3 mV/s using H_2SO_4 as an electrolyte

the mesopore size distributions of the RS and SC increased gradually; on the other hand, their mesopore volumes decreased significantly. The decrease in the mesopore volumes occurred because mesopores can provide more reaction sites with phosphoric acid, which results in the severe collapse of mesopore volume [42]. The phosphoric acid activation induces the chemical and structural alterations of the different constituent biopolymers of the precursors, namely cellulose, hemicellulose, and lignin, leading to the development of extensive porous structures.

For WNP 800 and CC 400, meso- and microporous surface areas are comparable. It is clear that WNP 800 and CC 400 exhibited a higher specific surface area and larger average pore size, as well as a larger pore volume than other samples. The reason for this is that the addition of the activating agent might cause a partial structural collapse and dissolution of the inorganic impurities, which are adverse for reducing the surface area and dissolving the non-carbons at lower temperatures. In all cases, thermal treatment of the acid-impregnated samples resulted in a decrease in the carbon content with respect to the raw precursors employed (Table 1). This effect could be associated with the cross-linking and aromatization reactions proceeding during the thermal treatment [43]. In addition, hydrolysis of polyester upon acid impregnation leading to a higher release of volatile compounds and fibre breakage, during the thermal treatment stage. The effect of activation

temperature may be explained using the mechanism of phosphoric acid activation [44]. Phosphoric acid acts as catalyst on the one hand promoting bond cleavage reactions, on the other hand facilitating cross-linking via cyclization, condensation, and forming phosphate and polyphosphate linkages. After the removal by washing, polyphosphates leave a space called pores. When activation temperature is increased by 900 and 500 °C, pore walls may thin to the point of disappearance causing BET surface area and pore volumes to decrease (Table 3). The deterioration of the porous structure is most probably due to the destruction of wall between adjacent micropores by reaction with phosphoric acid. The phosphoric acid decreases the formation of tars by catalyzing the alkylation of aromatic structures and oligomerization of alkenes and thus increasing the formation of a rigid cross-linked solid [44]. When the activation temperature is increased by 900 and 500 °C, the less amount off-gases are evolved and consequently the destruction of micropores was obtained. Thus, activation mechanism can be visualized as an interaction between the activating agent and the carbon atoms, which form the structure of the intermediate carbonized product resulting in useful large internal surface area with interconnected pores of desired dimension and surface chemical groups. These observations made clear that the activating agents at lower temperatures may contribute to pore drilling as well as pore widening effects, whereas at higher temperatures, the pore widening effects predominates the pore drilling forces [45].

3.5 Capacitor Performances

The effect of heat treatment on the electrochemical performance mainly depends on the temperature at which the material has been prepared in addition to the textural and chemical properties of the resulting carbon. The capacitors based on activated carbons 600–800 and also for cotton cloth 300–450 show the regular box-like voltammograms, with a steep current change at the switching potential and characteristic behaviour of an ideal capacitor. The rectangular shape is well conserved over a scan rate of 2–3 mV/s, which indicates the quick charge transmission. The heat treatment produces major changes in the electrical conductivity, considered by an important jump between 600 and 700 °C and followed by a further increase up to 800 °C.

Earlier investigations [46–48] shown that a conversion between an insulating and a conducting state usually occurs when carbon materials are heated around 600–700 °C, where as in the case of cloth fibre, it is 300–400 °C. Among sugarcane bagasse (4 a), rice straw (4 b), cotton cloth (4 c) and waste newspaper (4 d), cotton cloth (4 c) fibre shows the maximum conductivity, because of its high fibre content. The elimination of strong electron-withdrawing heteroatoms (primarily acidic functionalities) from the carbon surface favours the electron delocalization, and the electrical conductivity is remarkably improved. In case of CC, the conductivity increases rapidly by at least three orders of degree by heating at 400 °C. Above 400 °C, the much slower increase of the electrical conductivity is maybe related to the development in the structural order by thermal annealing of the pseudographitic carbonaceous layers [46–48] before to the loss of further surface groups.

Table 4 Sample code, surface area and their specific capacitance of cellulose carbons

Sample	Surface area (m^2/g)	Specific capacitance (F/g)
PCC (SC)	169.60	92
PCC (RS)	135.06	56
PCC (WNP)	336.09	105
PCC (CC)	581.34	130
SC 600	676.95	340
RS 600	376.65	112
WNP 800	1,104.08	380
CC 400	1,193.17	400

The total capacitance of the prepared carbons was calculated directly from the current–voltage curves as given below.

$$C = \left(\frac{I_a - I_c}{2v \cdot m}\right) = \left(\frac{\Delta I}{2v \cdot m}\right) \quad (5)$$

where C is specific capacitance (F/g), m, mass of the WNP carbon powder, v, potential scan rate (V/s), I_a and I_c, the average anodic and cathodic currents, respectively. To determine the capacitance as a function of potential, Δ I values were obtained at different potentials. The specific capacitance of the SC carbon electrodes be in the range 92–340 F/g, for RS, it was found to be 56–112 F/g, for WNP carbon electrodes is in the range of 105–380 F/g, whereas for CC electrodes, it was found to be 130–400 F/g at scan rates of 2–3 mV/s (Fig. 4).

Table 4 shows the BET surface area and their specific capacitance of the as prepared cellulose carbon materials. Generally, the specific capacitance of the carbon electrode will increase with increase in surface area of the carbon, and hence, higher surface area of SC 600 (676.95 m^2/g), RS 600 (396.03 m^2/g), WNP 800 (1,104.08 m^2/g) and CC 400 (1,193.17 m^2/g) gives capacitance of 340, 112, 380 and 400 F/g. The presence of macropores will also be a reason for the transportation of the electrolyte ions to the bulk materials. It is suggested that the ions can occupy some of the pores in the electrode to take part in the double-layer formation. As the scan rate increases, the square potential becomes gradually depressed because the ions transport into the pores more readily in lower scan rate than in higher. It was reported that the functional groups could increase the wettability of the electrode. Thus, the specific capacitance increases with

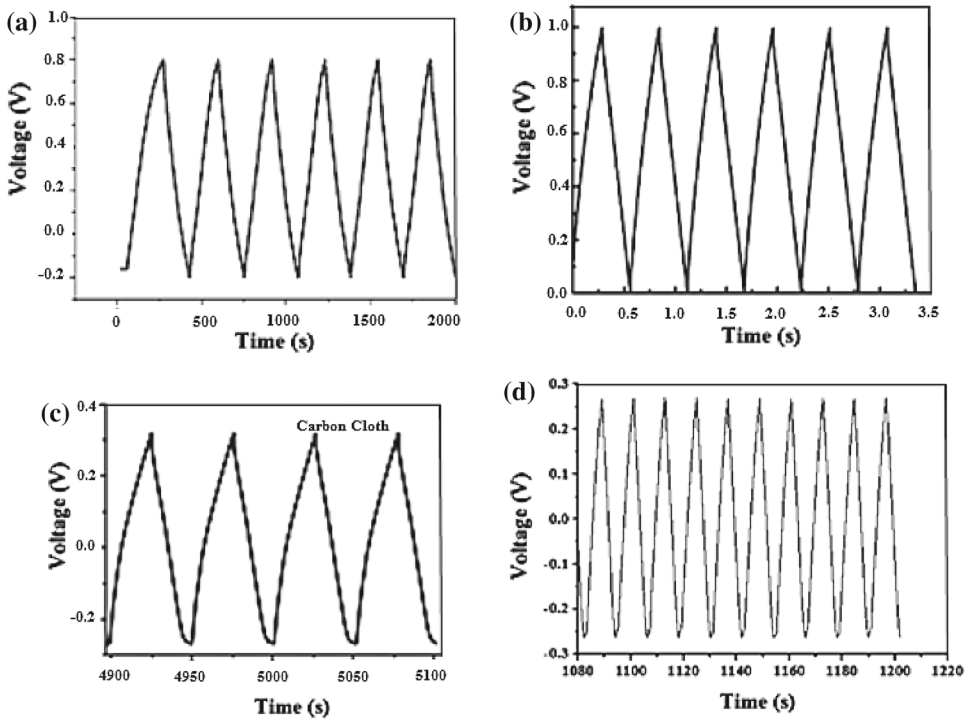

Fig. 5 Galvanostatic charge–discharge curve of **a** SC 600, **b** RS 600, **c** CC 400 and **d** WNP 600 carbon samples

Table 5 Cellulose materials from various agricultural residues used to prepare activated carbon for capacitor application [49]

S. no.	Biomass material	Activating agent	Electrolyte	Surface area (m^2/g)	Specific capacitance (F/g)
1	Rice Husk	NaOH	KCl	1,886	210
2	Wheat straw	KOH	$MeEt_3NBF_4/CH_3CN$	2,316	25
3	Banana fiber	$ZnCl_2$	Na_2SO_4	686	74
4	Sunflower	KOH	KOH	1,371	311
5	Sorghum pitch	NaOH	H_2SO_4	17	220

increase in BET surface area of the carbon electrode. The galvanostatic charge–discharge behaviour is studied for SC 600, RS 600, WNP 800 and CC 400 alone. Figure 5a–d shows the ultrafast charge–discharge rate and linear dependence on voltage as well as time with a very small voltage drop. These results indicate that the SC 600, RS 600, WNP 800 and CC 400 used in the present work exhibit exceptional supercapacitor performance than the reported (Table 5). Thus, these results obviously indicate the ideal double-layer behaviour and the excellent supercapacitor performance of cellulose materials as an electrode material for energy storage devices [37].

4 Conclusions

The electron transport properties of cellulose materials were studied in detail along with their microstructure. The presence of the graphitic layer has been confirmed from the X-ray diffraction pattern. It was found that the chemical activation at 600, 800 and 400 °C is the optimum to produce a high porous carbon and is confirmed by SEM analysis. The gradual development of the electrochemical performances of carbon-based capacitors at high current densities, subsequent heat treatments up to 800 °C is mainly due to the effect of simultaneous increase in conductivity. These properties possibly enable these cellulosic wastes to act as a source of carbonaceous materials for the development of ideal high-performance supercapacitors.

Acknowledgments The corresponding author duly acknowledge the financial support rendered by SERC Division, Department of Science and Technology (DST), New Delhi, India, through the young scientist project scheme vide reference No. SR/FTP/PS-76/2005.

References

1. Spain, I.L.: In: Walker, P,L; Thrower, P.A, (eds.). Chem. Phys. Carbon, Marcel Dekker New York (1994)
2. Gonzalez, J.S.; Garia, A.M.: Electrical conductivity of carbon blacks under compression. Carbon **43**, 741–747 (2005)
3. Tans, S.J.; Devoret, M.H.; Dal, H.: Individual single-wall carbon nanotubes as quantum wires. Nature **386**, 474–477 (1997)

4. Mrozowski, S.: In: Proceedings 3rd Carbon Conference, Buffalo, USA (1957)
5. Holm, R.: Electrical Contacts. H Geben, Stockholm (1946)
6. Imasogie, B.I.; Wendt, U.: Characterization of graphite particle shape in spheroidal graphite iron using a computer-based image analyzer. J. Miner. Mater. Charact. Eng. **3**, 1–12 (2004)
7. Kinoshita, K.: Electrochemical and Physical Properties, Carbon, Chapter 2.5. Wiley, New York (1988)
8. Pantea, D.; Darmstadt, H.; Kaliaguine, S.: Electrical conductivity of thermal carbon blacks: influence of surface chemistry. Carbon **39**, 1147–1158 (2001)
9. Pantea, D.; Darmstadt, H.; Kaliaguine, S.: Electrical conductivity of conductive carbon blacks: influence of surface chemistry and topology. Appl. Surf. Sci. **217**, 181–193 (2003)
10. Cheol-Min, Y.; Yong-Jung, K.; Morinobu, E.: Nanowindow-regulated specific capacitance of supercapacitor electrodes of single-wall carbon nanhorns. J. Am. Chem. Soc. **129**, 20–21 (2007)
11. Saito, Y.; Tsujimoto, Y.; Koshio, A.: Field emission patterns from multiwall carbon nanotubes with a cone-shaped tip. Appl. Phys. Lett. **90**, 213108-3 (2007)
12. Sanchez, G.R.; Bruno, M.M.; Thomas, Y.R.J.: Mesoporous carbon supported nanoparticulated $PdNi_2$: a methanol tolerant oxygen reduction electrocatalyst. Int. J. Hydrogen Energy **37**, 31–40 (2012)
13. Pagona, G.; Tagmatarchis, N.; Fan, J.: Cone-end functionalization of carbon nanohorns. Chem. Mater. **18**, 3918–3920 (2006)
14. Klemm, D.; Philipp, B.; Heinze, T.: Comprehensive Cellulose Chemistry. Wiley VCH, Chichester (1998)
15. Angin, D.: Utilization of activated carbon produced from fruit juice industry solid waste for the adsorption of Yellow 18 from aqueous solutions. Bioresour. Technol. (2014). doi:10.1016/j.biortech.2014.02.100
16. Juan, C.M.P.; Liliana, G.: Comparison of the oxidation of phenol with iron and copper supported on activated carbon from coconut shells. Arab. J. Sci. Eng. **38**(1), 49–57 (2013)
17. Amrita, J.; Tripathi, S.K.: Fabrication and characterization of energy storing supercapacitor devices using coconut shell based activated charcoal electrode. Mater. Sci. Eng.B **183**, 54–60 (2014)
18. Mussatto, S.I.; Teixeira, J.A.: Lignocellulose as raw material in fermentation processes. In: Méndez-Vilas, A. (ed.) Current Research, Technology and Education Topics in Applied Microbiology and Microbial Biotechnology, vol 2, pp. 897–907. Formatex Research Center, Badajoz (2010)
19. Daud, W.M.A.W.; Ali, W.S.W.; Sulaiman, M.Z.: The effects of carbonization temperature on pore development in palm-shell-based activated carbon. Carbon **38**, 1925–1932 (2000)
20. Suhas, P.J.M.; Carrott, M.M.L.; Carrott, R.: Lignin—from natural adsorbent to activated carbon: a review. Bioresour. Technol. **98**, 2301–2312 (2007)
21. Kumar, K.S.; Huerta, G.V.; Castellanos, A.R.: Microwave assisted synthesis and characterizations of decorated activated carbon. Int. J. Electrochem. Sci. **7**, 5484–5494 (2012)
22. Toles, C.A.; Marshall, W.E.; Johns, M.M.; Lynda, H.; Wartelle, L.H.; McAloon, A.: Acid-activated carbons from almond shells: physical, chemical and adsorptive properties and estimated cost of production. Bioresour. Technol. **71**, 87–92 (2000)
23. Fierro, V.; Fernandez, T.V.; Celzard, A.: Study of the decomposition of kraft lignin impregnated with orthophosphoric acid. Thermochim. Acta **433**, 142–148 (2005)
24. Montane, D.; Fernandez, T.V.; Fierro, V.: Activated carbons from lignin: kinetic modeling of the pyrolysis of Kraft lignin activated with phosphoric acid. J. Chem. Eng. Data **106**, 1–12 (2005)
25. Trassl, S.; Motz, G.; Rossler, E.; Ziegler, G.: Characterisation of the free-carbon phase in precursor-derived SiCN ceramics. J. Non-Cryst. Solids **293**, 261–267 (2001)
26. Holm, R.: In: Electric Contacts: Theory and Applications. Springer, Berlin (1967)
27. Donnet, J.B.; Voet, A.: Carbon Black: Physics, Chemistry, and Elastomer Reinforcement. Marcel Dekker, New York (1976)
28. Celzard, A.; Mareche, J.F.; Payo, F.: Electrical conductivity of carbonaceous powder. Carbon **40**, 2801–2815 (2001)
29. Pastor, A.C.; Rodriguez, R.; Marsh, R.H.: Preparation of activated carbon cloths from viscous rayon. Part I. Carbonization procedures. Carbon **37**, 1275–1283 (1999)
30. Liao, L.; Wu, C.; Yanyongjie, Y.: Chemical elemental characteristics of biomass fuels in China. Biomass. Bioenerg. **27**, 119–130 (2004)
31. Van Soest, P.J.: Rice straw, the role of silica and treatments to improve quality Anim. Feed. Sci. Technol. **130**, 137–171 (2006)
32. Raveendran, K.; Anuraddha, G.; Kartick, C.: Influence of mineral matter on biomass pyrolysis characteristics. Fuel **74**, 1812–1822 (1995)
33. Yalcin, N.; Sevnic, V.: Studies on silica obtained from rice husk. Ceram. Int. **27**, 219–224 (2001)
34. Wang, T.H.; Tan, S.X.; Liang, C.H.: Using oxidation to increase the electrical conductivity of carbon nanotube electrodes. Carbon **47**, 1867–1870 (2009)
35. Inagaki, M.: Pores in carbon materials-importance of their control. New Carbon Mater. **24**, 193–232 (2009)
36. Parikh, D.V.; Thibodeaux, D.P.; Condon, B.: X-ray crystallinity of bleached and crosslinked cottons. Text. Res. J. **77**, 612–616 (2007)
37. Adinaveen, T.; Kennedy, L.J.; Vijaya, J.J.: Studies on structural, morphological, electrical and electrochemical properties of activated carbon prepared from sugarcane bagasse. J. Ind. Eng. Chem. **19**, 1470–1476 (2013)
38. Senthilkumar, S.T.; Senthilkumar, B.; Balaji, S.: Preparation of activated carbon from sorghum pith and its structural and electrochemical properties. Mater. Res. Bull. **46**, 413–419 (2011)
39. Dubinin, M.M.; Serpinsky, V.V.: Isotherm equation for water vapour adsorption by microporous carbonaceous adsorbents. Carbon **19**, 402–403 (1981)
40. Guo, Y.; Yang, Y.; Wang, Z.: The preparation and mechanism studies of rice husk based porous carbon. Mater. Chem. Phys. **74**, 320–323 (2002)
41. Fierro, V.; Muniz, G.; Basta, A.H.; El-Saied, H.; Celzard, A.: Rice straw as precursor of activated carbons: activation with orthophosphoric acid. J. Hazard. Mater. **181**, 27–32 (2010)
42. Jeong, E.; Jung, M.J.; Lee, Y.K.: Role of fluorination in improvement of the electrochemical properties of activated carbon nanofiber electrodes. J. Fluor. Chem. **150**, 98–103 (2013)
43. Derbyshire, F.; Jagtoyen, M.; Thwaites, M.: In: Patrick, J.W. (ed.) Activated Carbons-Production and Application. Halsted Press, pp. 227–252 (1995)
44. Jagtoyen, M.; Derbyshire, F.: Activated carbons from yellow poplar and white oak by H_3PO_4 activation. Carbon **36**, 1085–1097 (1998)
45. Tsai, W.T.; Chang, C.Y.; Lin, M.C.; Chien, S.F.; Sun, H.F.; Hsieh, M.F.: Adsorption of acid dye onto activated carbons prepared from agricultural waste bagasse by $ZnCl_2$ activation. Chemosphere **45**, 51–58 (2001)
46. Spain, I.L.: Electronic transport properties of graphite, carbons, and related materials. In: Walker, P.L. Jr.; Thrower, P.A. (eds.) Chemistry and Physics of Carbon, Marcel Dekker, New York (1981)
47. Marchand, A.; Figueiredo, J.L.; Moulijn, J.A.: Carbon and Coal Gasification. Martinus Nijhoff, Dordrecht (1986)
48. Leon, Y.C.A.; Radovic, L.R.: Interfacial chemistry and electrochemistry of carbon surfaces. In: Thrower, P. (ed.) Chemistry and Physics of Carbon, Marcel Dekker, New York (2001)
49. Kalyani, P.; Anitha, A.: Biomass carbon & its prospects in electrochemical energy, systems. Int. J. Hydrogen Energy **38**, 4034–4045 (2013)